

Dynamic behavior of metal nanoparticles in MOF materials: analysis with electron microscopy  
and deep learning

Erokhin K.S.,<sup>a,c</sup> Pentsak E.O.,<sup>a,c</sup> Sorokin V.R.,<sup>b</sup> Agaev Yu.V.,<sup>b</sup> Zaytsev R.G.,<sup>b</sup> Isaeva V.I.,<sup>a</sup>  
Ananikov V.P.<sup>a,b\*</sup>

<sup>a</sup>Zelinsky Institute of Organic Chemistry, Russian Academy of Sciences, Leninsky Prospect, 47, Moscow, 119991, Russia;  
<https://AnanikovLab.ru>

<sup>b</sup> Platov South-Russian State Polytechnic University (NPI), Prosveschenia Str. 132, Novocherkassk 346428, Russia

<sup>c</sup> The authors contributed equally

Table of Content

1. TEM analysis of MOF materials .....	2
2. TGA analysis.....	5
3. Powder XRD analysis .....	6
4. Analysis with HR-TEM .....	10
5. SAED analysis.....	12
References .....	13

## 1. TEM analysis of MOF materials

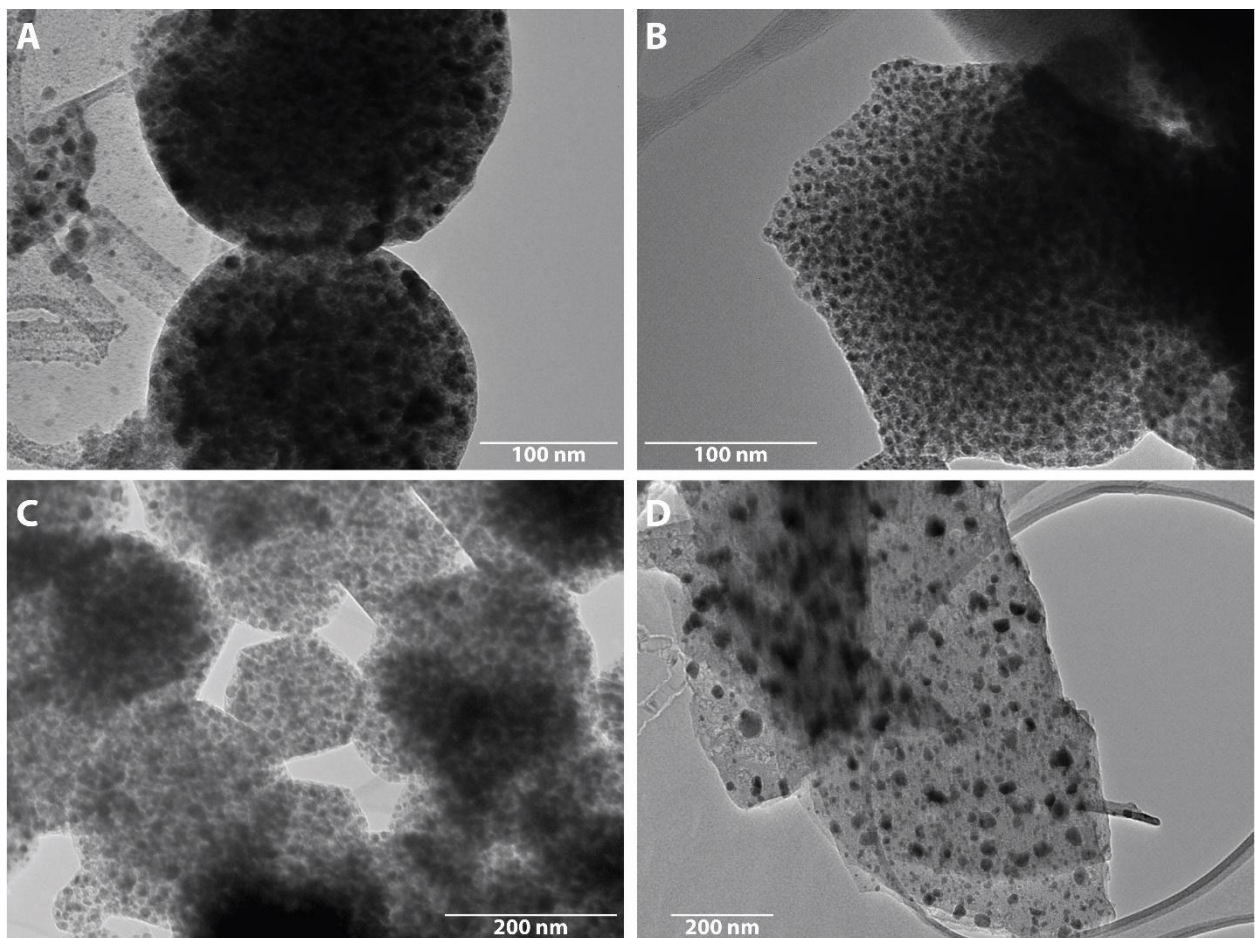


**Figure S1.** TEM images of MOFs, which are unstable under an electron beam: (A) MIL-101(Fe); (B) NH<sub>2</sub>-MIL-101(Fe); (C) ZIF-67(Co); (D) BIF-66(Co). Electron beams cause MOF decomposition and the formation of nanoparticles.

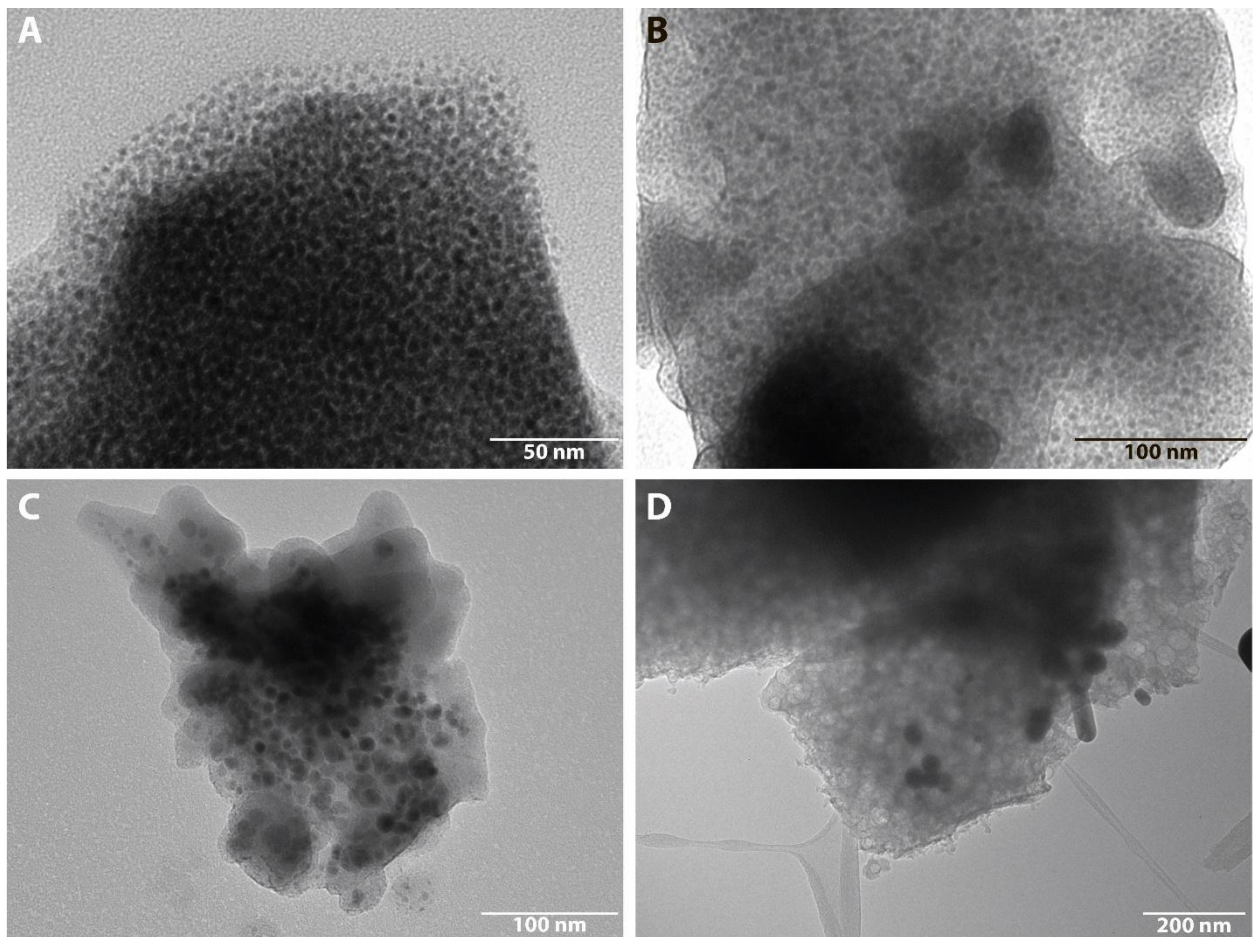


**Figure S2.** TEM images of MOFs unstable under an electron beam: (A) Ni(BDC); (B) Ni(BTC); (C) MOF-74(Ni); (D) HKUST-1(Cu). Electron beams cause MOF decomposition and the formation of M-NP.

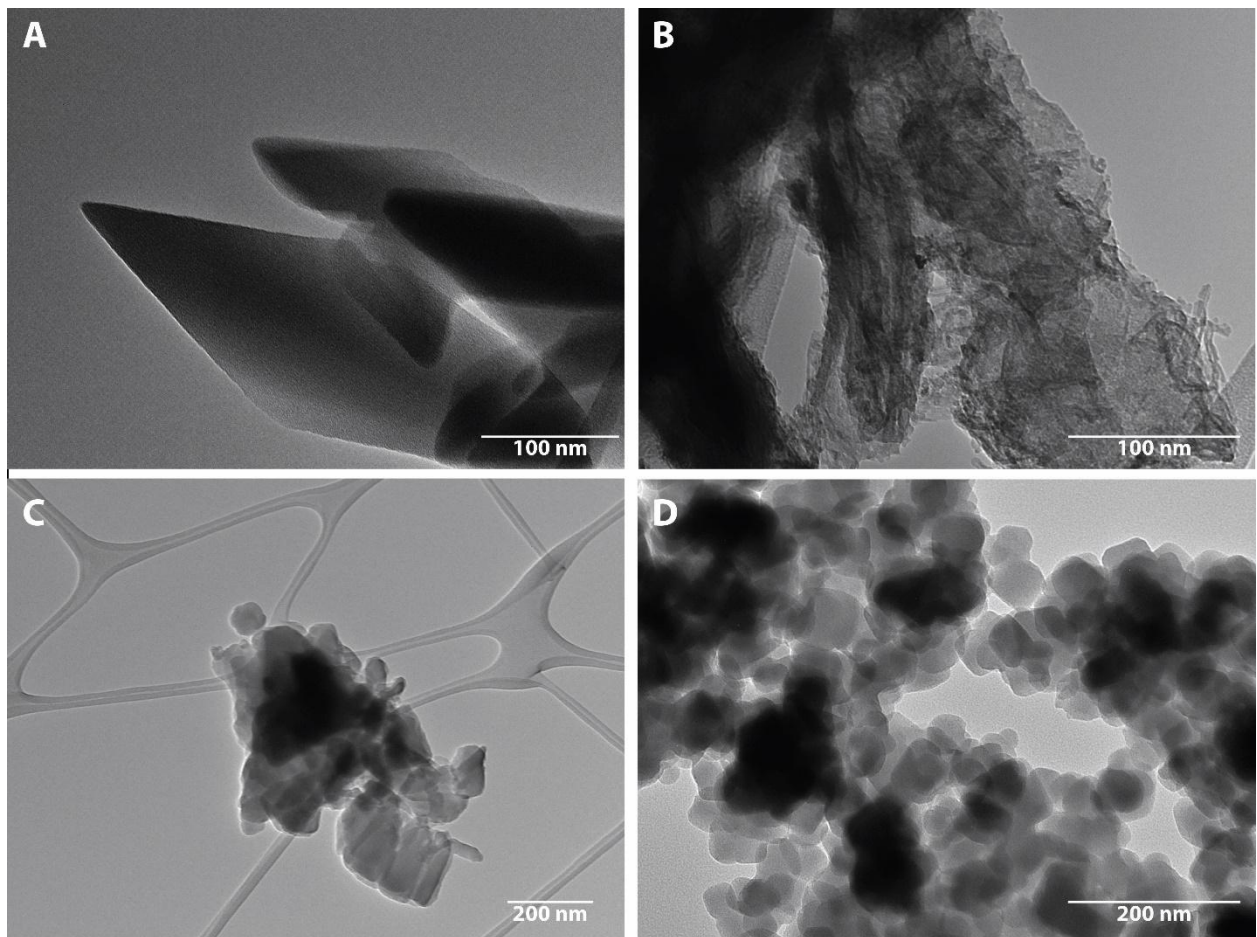


**Figure S3.** TEM images of MOFs stable under an electron beam: (A) MIL-53(Al); (B) NH<sub>2</sub>-MIL-53(Al); (C) NH<sub>2</sub>-MIL-101(Al); (D) ZIF-8(Zn).

## 2. TGA analysis

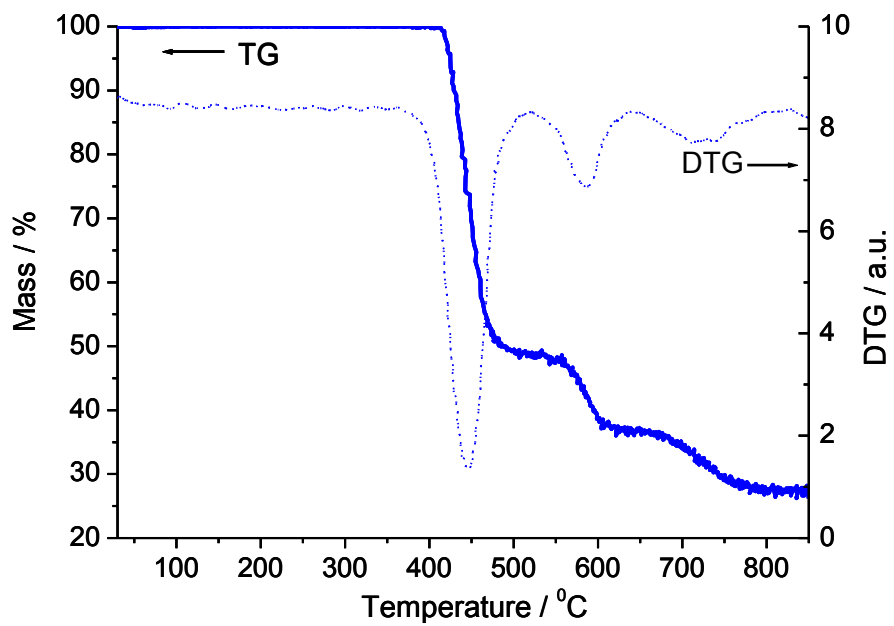


**Figure S4.** TG, DTG curves for sample BIF-66.

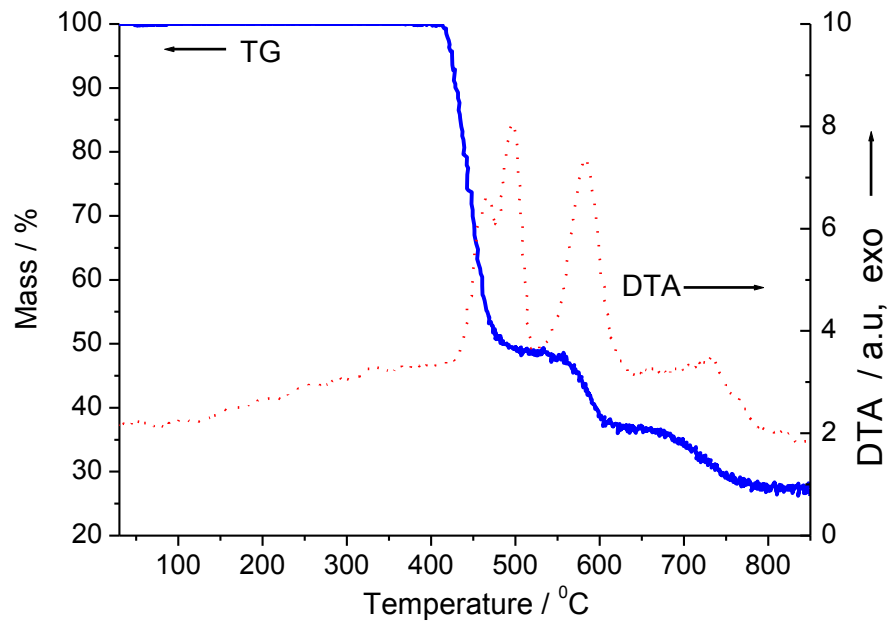


**Figure S5.** TG, DTA curves for sample BIF-66.

### 3. Powder XRD analysis

For MOF samples MIL-53(Al), NH<sub>2</sub>-MIL-101(Al), NH<sub>2</sub>-MIL-53(Al), ZIF-8(Zn), MIL-101(Fe), NH<sub>2</sub>-MIL-101(Fe), BIF-66, ZIF-67, and HKUST-1, X-ray powder diffraction data were collected (22°C) in a reflection mode utilizing a Panalytical EMPYREAN instrument equipped with a linear X'celerator detector and non-monochromated Ni-filtered Cu K<sub>α</sub> radiation ( $\lambda=1.5418 \text{ \AA}$ ). Measurement parameters are as follows: tube voltage/current 45 kV / 40 mA, divergence slits of 1/8 and 1/4°, 2θ range 3-40°, speed 1° min<sup>-1</sup>.

PXRD patterns of NiBTC and MOF-74(Ni) were collected with a diffractometer DRON-2 using the following mode: 2Θ=10-60° range, rate 1°/min, Cu K<sub>α</sub> radiation (30 kV, 30 mA), Ni-filter.

Micro-powder X-ray diffraction was used for NiBDC analysis and was carried out on a four-circle Rigaku Synergy S diffractometer equipped with a HyPix6000HE area-detector (kappa geometry, shutterless ω-scan technique), using monochromatized Cu K<sub>α</sub> radiation (50 kV, 1 mA). Samples were fixed on the loop utilizing grease (Dow corning). Data were collected at 22°C, exposure time was 300 s and detector distance was 120 mm in 2θ range 0-50°.

XRD patterns of the synthesized MOF samples, i.e., NH<sub>2</sub>-MIL-101(Al), BIF-66, ZIF-67, HKUST-1, NiBTC, and MOF-74(Ni) are consistent with those reported in literature.<sup>1-4</sup>

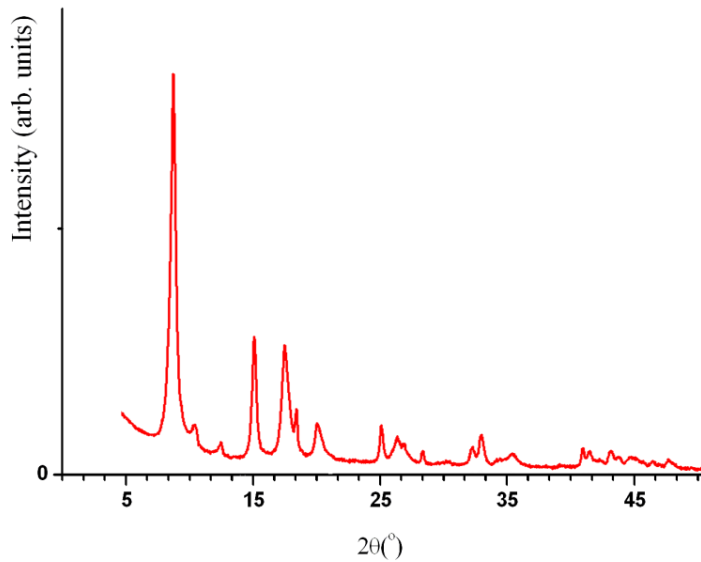


**Figure S6.** PXRD pattern of MIL-53(Al).

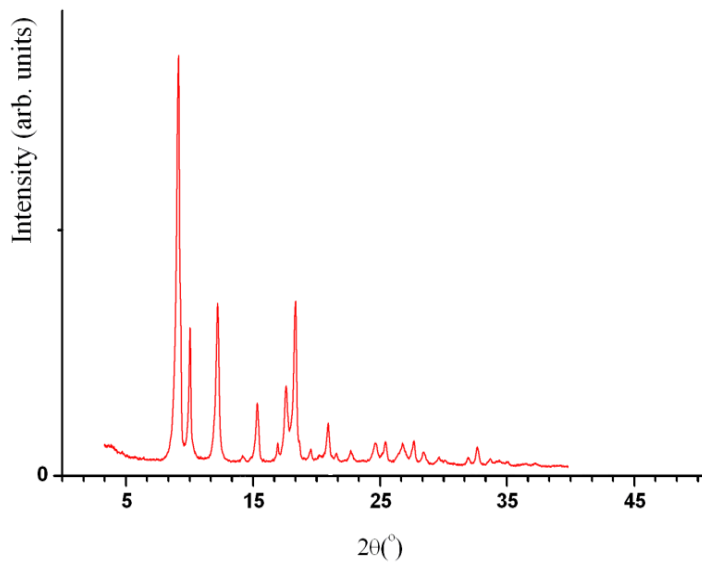


**Figure S7.** PXRD pattern of  $\text{NH}_2\text{-MIL-53(Al)}$ .

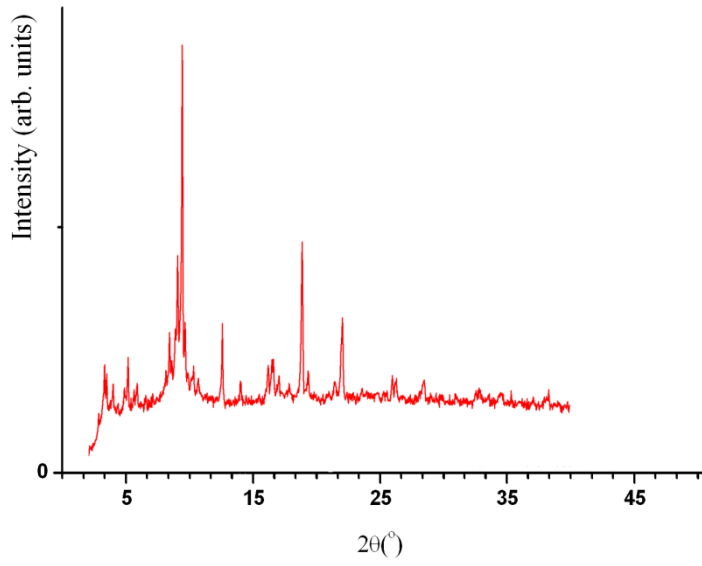


**Figure S8.** PXRD pattern of  $\text{MIL-101(Fe)}$ .

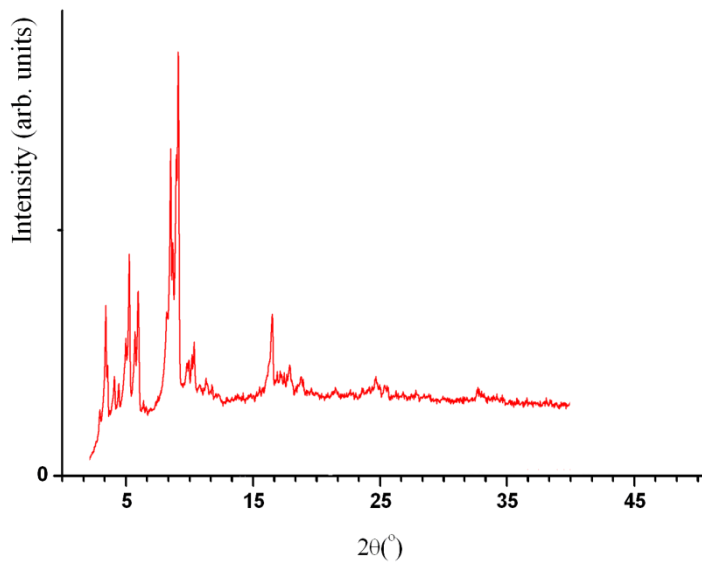


**Figure S9.** PXRD pattern of  $\text{NH}_2\text{-MIL-101(Fe)}$

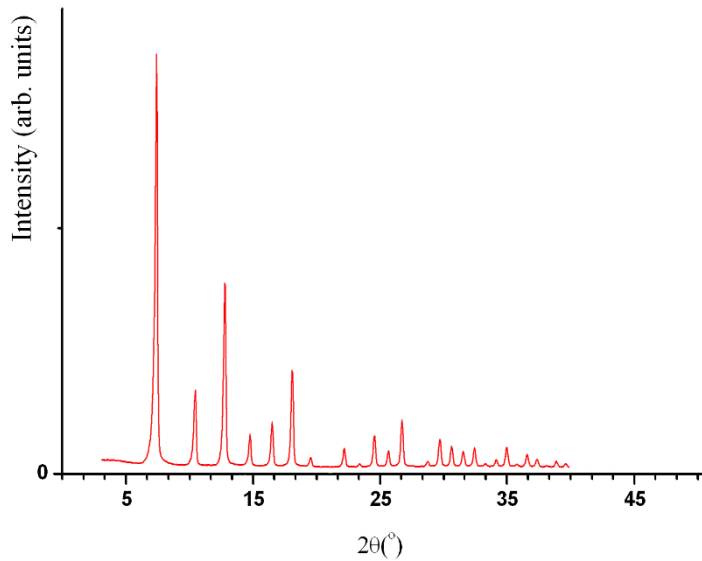


**Figure S10.** PXRD pattern of ZIF-8.

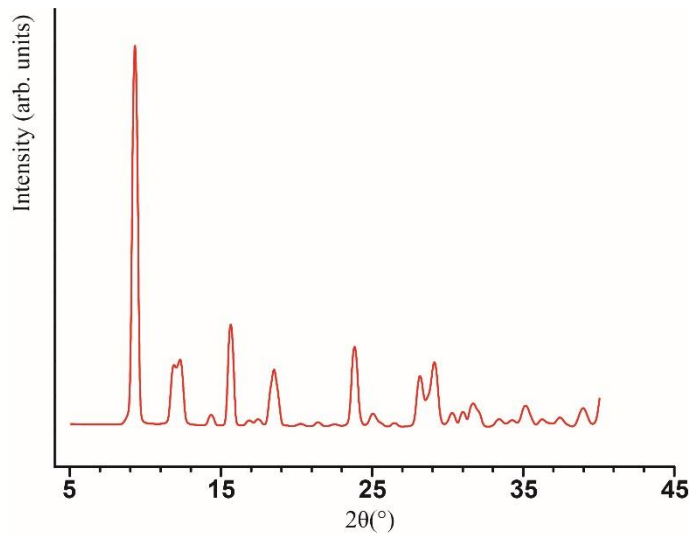


**Figure S11.** PXRD pattern of NiBDC.

#### 4. Analysis with HR-TEM

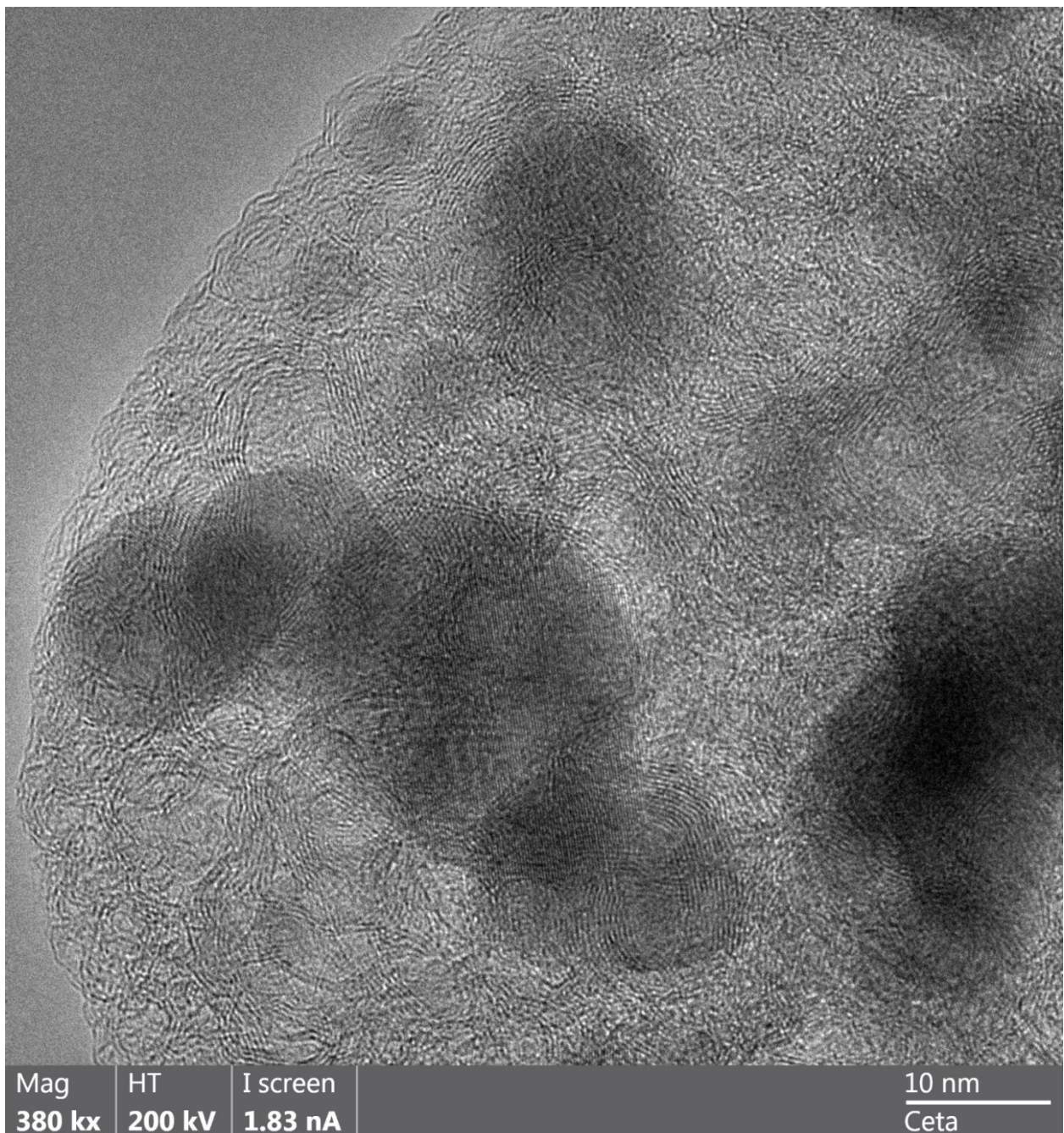
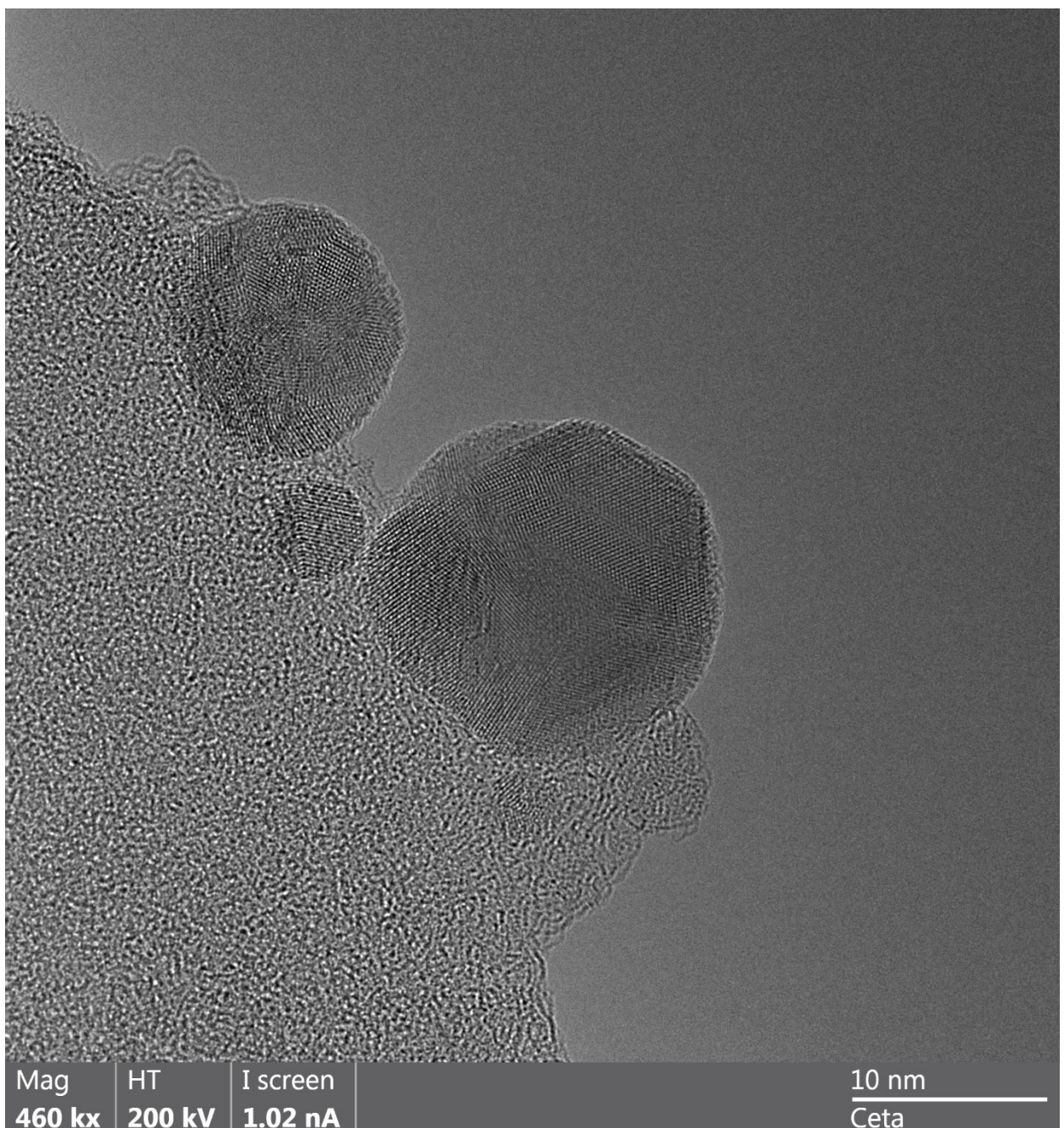


**Figure S12.** HR-TEM image of ZIF-67 with formed Co NPs.



Mag  
**460 kx**

HT

**200 kV**

I screen

**1.02 nA**

10 nm

Ceta

**Figure S13.** HR-TEM image of HKUST-1 with formed Cu NPs.

## 5. SAED analysis

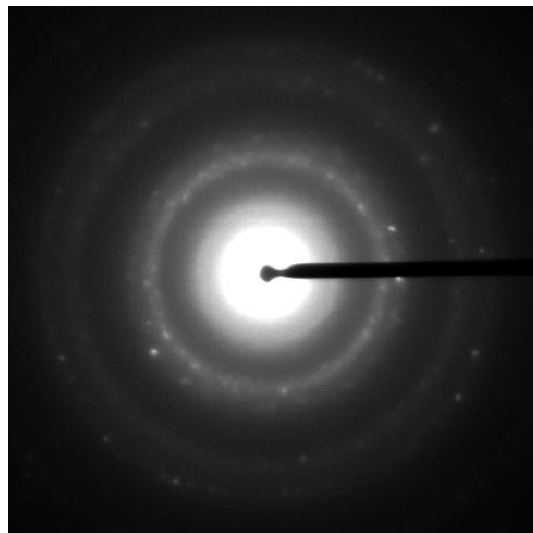


**Figure S14.** ED pattern of ZIF-67 particle with formed Co NPs.

## References

1. V. I. Isaeva, M. N. Timofeeva, I. A. Lukoyanov, E. Y. Gerasimov, V. N. Panchenko, V. V. Chernyshev, L. M. Glukhov and L. M. Kustov, *J. CO<sub>2</sub> Util.*, 2022, **66**, 102262.
2. G. S. Deyko, L. M. Glukhov, V. I. Isaeva, V. V. Chernyshev, V. V. Vergun, D. A. Archipov, G. I. Kapustin, O. P. Tkachenko, V. D. Nissenbaum and L. M. Kustov, *Crystals*, 2022, **12**, 279.
3. V. I. Isaeva, K. Papathanasiou, V. V. Chernyshev, L. Glukhov, G. Deyko, K. K. Bisht, O. P. Tkachenko, S. V. Savilov, N. A. Davshan and L. M. Kustov, *ACS Appl. Mater. Interfaces*, 2021, **13**, 59803-59819.
4. E. S. Degtyareva, K. S. Erokhin and V. P. Ananikov, *Catal. Commun.*, 2020, **146**, 106119.